JOURNAL OF COMPUTATIONAL PHYSICS **135,** 83–96 (1997)
ARTICLE NO. CP975741

On the Coupling of Aerodynamic and Structural Design

Eyal Arian

Institute for Computer Applications in Science and Engineering (ICASE), NASA Langley Research Center, Hampton, Virginia 23681-0001
E-mail: arian@icase.edu

Received December 1, 1995; revised November 26, 1996

The symbol of the Hessian for a static aeroelastic optimization model problem is analyzed for the optimization of a plate's shape and rigidity distribution with respect to a given cost function. The flow is modeled by the small-disturbance full-potential equation and the structure is modeled by an isotropic (von Kármán) plate equation. The cost function consists of both aerodynamic and structural terms. In the new analysis the symbol of the cost function Hessian near the minimum is approximated for the nonsmooth error components in the shape and rigidity. The result indicates that the system can be decoupled to two single discipline subminimization problems which will effectively converge to the multidisciplinary optimal solution. The result also indicates that the structure part in the Hessian is well conditioned while the aerodynamic part is ill conditioned. Applications of the result to optimization strategies are discussed and demonstrated numerically.

1. INTRODUCTION

Lately, there is a growing interest in multidisciplinary design and optimization (MDO) [1–4]. An important problem in that field is the static aeroelastic optimal design problem (for example, [5–7]). In this problem there are two coupled disciplines: aerodynamics and structural analysis. The problem is to compute the aerodynamic shape and structural rigidity such that some given cost function is minimized.

The purpose of this paper is to demonstrate new analysis of Hessians for MDO problems on the above aeroelastic optimization problem and to draw some practical conclusions. The approach is to consider a simple model problem and approximate the symbol of the Hessian near the minimum for the nonsmooth frequencies. The Hessian contains curvature information which is essential for the solution of ill-conditioned optimization problems. Hessian symbols were previously computed for smoothing predictions in the development of multigrid one-shot methods [8–11] and lately for the analysis of inviscid aerodynamic optimization problems [12]. The analysis in this paper indicates that for the nonsmooth components the system can be decoupled to two single discipline subminimization problems which will effectively converge to the multidisciplinary optimal solution. The analysis also indicates that the structures part in the Hessian is well conditioned while the aerodynamics part is ill conditioned. It should be emphasized that in this study the shape of the plate is allowed to change only in the normal direction (the planform remains fixed). Therefore, no inferences could be made as to the coupling between the aerodynamic and the structural design when the planform's shape is allowed to change during the optimization.

One consequence of this result is that the solution of such problems can be achieved in two stages. In the first stage, the MDO approach should be taken on a coarse model; that is, the flow and the structure equations are considered simultaneously during the minimization, which is a more complex problem than optimizing the decoupled individual disciplines problems. In the second stage, a refined CFD code for the flow and a detailed finite element code for structure should be used in a sequential algorithm in which the shape is optimized relative to aerodynamic considerations, followed by structural optimization limited to a given shape. This approach should result in a good approximation of the multidisciplinary optimal solution.

The paper outline is as follows. In Section 2 the optimization problem is formulated. In Section 3 the necessary conditions for a minimum are derived with the adjoint method and their relation with the Hessian is discussed. In Section 4 the symbol of the Hessian for the nonsmooth frequencies is derived by using local mode analysis. In Section 5 applications of the result to optimization strategies are discussed. In Section 6 the two strategies are demonstrated numerically on a simple model problem. Finally, Section 7 contains concluding remarks.

2. PROBLEM FORMULATION

In this section the aeroelastic analysis problem and the optimal design problem are presented. The aeroelastic analysis problem couples the full-potential flow equation with the isotropic von Kármán plate equation to give the pressure distribution over the plate, p, and the plate deformation, W, for a given plate shape, α, and rigidity distribution, D. The design problem is to compute the "best"

0021-9991/97 $25.00

shape and structural rigidity so that a given cost function is minimized.

The cost function is composed of aerodynamic and structure parts. The aerodynamic cost function estimates performance by measuring the difference, in L_2 norm, of the pressure distribution from a desired one. The structure cost function gives a measure of the structural weight and penalizes structural deformation.

Since our interest is in a local mode analysis of the Hessian near the minimum, we consider the small disturbance equations of flow over a flat plate.

2.1. The Flow Model

We choose the full-potential equation as a model for the flow. It approximates inviscid flow characteristics and is used in applications for aerodynamic optimal design (for example, [13]). For the analysis of the cost function's Hessian in the vicinity of the minimum it is enough to consider small perturbations of the shape from the optimal solution. The resulting changes in the potential, ϕ, satisfy the steady state small disturbance potential equation. The geometry is taken to be half-space $\Omega = (x, y, z \geq 0)$, where the x axis is the stream-wise coordinate, y is the coordinate perpendicular to the stream and parallel to the plate (spanwise direction), and z is in the normal direction to the plate.

The aerodynamic state equation.

$$\begin{aligned} &\mathbf{L}\phi = 0 \quad z \geq 0 \\ &\mathbf{B}\phi = (\alpha_x + W_x) \quad z = 0 \end{aligned} \tag{2.1}$$

with the following definitions of the interior operator, **L**, and boundary operator, **B**

$$\begin{aligned} &\mathbf{L} = (1 - M^2)\partial_{xx} + \partial_{yy} + \partial_{zz} \\ &\mathbf{B} = \partial_z, \end{aligned} \tag{2.2}$$

where U_∞ is the free stream velocity, M is the Mach number, with the following far-field boundary conditions:

Inflow boundary condition.

Subsonic: $\phi_x = 0$
Supersonic: $\phi_x = 0$ and $\phi = 0$ (we assume that the normal free stream velocity, V_∞, is zero).

Outflow boundary condition.

Subsonic: $\phi_x = 0$
Supersonic: No Boundary Condition.

The missing low-order terms in the boundary condition of (2.1) vanish if the analysis is performed around a flat shape.

2.2. The Structural Model

The structural model consists of the isotropic von Kármán plate equation for the displacement W [14, 15]

$$\mathbf{G}(D, W) = -p \quad z = 0 \tag{2.3}$$

with the following definition of the operator **G**:

$$\begin{aligned} \mathbf{G}(D, W) = (DW_{xx})_{xx} + (DW_{yy})_{yy} + \nu[(DW_{yy})_{xx} \\ + (DW_{xx})_{yy}] + 2(1 - \nu)(DW_{xy})_{xy}, \end{aligned} \tag{2.4}$$

where D is the plate rigidity distribution, ρ_∞ is the flow density and ν is the Poisson ratio. The pressure, p, is related with the potential, ϕ, by the Bernoulli relation (we assume $\phi_x \ll U_\infty$)

$$p = p_\infty - \rho_\infty U_\infty^2 \phi_x. \tag{2.5}$$

In two space dimensions Eq. (2.3) reduces to the beam equation

$$(DW_{xx})_{xx} = -p_\infty + \rho_\infty U_\infty^2 \phi_x \quad z = 0. \tag{2.6}$$

There are few choices for the boundary conditions for the plate. However, Eq. (2.3) is elliptic, so the effect of a high-frequency error component in the deflection W is local, and therefore the plate boundary conditions do not play a role in the local mode analysis.

2.3. The Cost Function Model

The definition of the cost function is not unique and depends on the specific application under consideration. In general, the requirement of the aeroelastic optimal design is that it have maximum aerodynamic performance and minimum structural weight and deformation. Some of the desired features of the final design are in many cases modeled by a set of inequality constraints, as is the case for the minimum deformation requirement. However, for the purpose of this paper we will avoid inequality constraints by adding a term to the cost function which penalizes deformation. In the following the different terms composing the cost function are discussed.

- *The Aerodynamic Performance Term*

A common aerodynamic cost function is drag (or drag over lift). However, in inviscid aerodynamic optimization models a commonly used cost function is pressure matching (for example, [16–20]). Relation (2.5) implies the cost function term

$$F^{aero} = \int_\Gamma (\phi_x - f^*)^2 \, d\sigma,$$

TABLE I

Rigidity and Weight

	D	Weight
Beam	$\frac{Ebh^3}{12}$	$\rho_p \int_\Gamma bh\, dx$
Plate	$\frac{Et^3}{12(1-\nu^2)}$	$\rho_p \int_\Gamma t\, dx\, dy$

where $d\sigma$ is an integration element on the shape Γ. The target distribution, $f^*(x, y) \in L_2(\Gamma)$, is related to the desired pressure distribution, $p^*(x, y)$, by the relation

$$f^*(x, y) = \frac{p^*(x, y) - p_\infty}{-\rho_\infty U_\infty^2}.$$

- *The Structural Weight Term*

Another important factor in aeroelastic design is the resulting weight of the structure. In practice the weight is measured by the sum of the weights of all the components composing the structure. In plate models the weight is related with the plate rigidity, D, and is given in Table I, where E is the Young modulus of elasticity, b and h are the cross section components of the beam, ρ_p is the structural density, and t is the plate's thickness.

In both cases the weight of the structure is proportional to $D^{1/d}$ where d is the space dimension

$$F^{weight} \propto \int_\Gamma D^{1/d}\, d\sigma.$$

- *The Structural Deformation Term*

As a result of the pressure, p, exerted on the plate by the flow, the structure will deform its shape by W (bend and twist). In practice the structure is designed so that the amount of deformation will be constrained not to exceed some given limits. In this model we account for this requirement by penalizing the deformation which is measured by the work of the aerodynamic pressure on the plate, pW. This will add to the cost function the term (see Eq. (2.5))

$$F^{deform} = \rho_\infty U_\infty^2 \int_\Gamma \phi_x W\, d\sigma.$$

Note that the effect of transverse velocities have been disregarded in this model problem.

2.4. The Optimization Problem

We define the cost function, $F = F(\phi, W, D)$, to be

$$F(\phi, W, D) = \gamma_1 \int_\Gamma (\phi_x - f^*)^2\, d\sigma + \gamma_2 \int_\Gamma D^{1/d}\, d\sigma + \gamma_3 \int_\Gamma \phi_x W\, d\sigma, \tag{2.7}$$

where γ_1, γ_2, γ_3 are parameters. The cost function is a map from a function space to $\mathbb{R}$.

The minimization problem is to find a shape function, α, and rigidity distribution, D, such that the cost function is minimized subject to Eqs. (2.1) and (2.3). We assume the existence of a solution for both the state equations and for the optimization problem (a rigorous treatment of existence and uniqueness of solutions is beyond the scope of this paper).

3. ADJOINT FORMULATION AND THE HESSIAN

In this section the necessary conditions for a minimum are derived with the adjoint method (e.g., [17–22]). The necessary conditions are given as a set of state equations (the analysis problem), costate equations (the adjoint problem), and design equations (optimality conditions). Then the relation between the design equation residuals and the Hessian of the cost function is discussed. This relation will be used in the next section to derive the Hessian's symbol.

3.1. The Necessary Conditions for a Minimum

The Lagrangian is a functional defined by

$$\begin{aligned}\mathcal{L}(\phi, W, \alpha, D, \xi, \lambda, \eta) = F(\phi, W, D) &+ \int_\Gamma \xi(\mathbf{B}\phi - (\alpha_x + W_x))\, d\sigma \\ &+ \int_\Omega \lambda \mathbf{L}\phi d\Omega + \int_\Gamma \eta(\mathbf{G}(D, W) \\ &- \rho_\infty U_\infty^2 \phi_x)\, d\sigma,\end{aligned} \tag{3.1}$$

where $\xi = \xi(x, y)$, $\eta = \eta(x, y)$ and $\lambda = \lambda(x, y, z)$ are Lagrange multipliers. The first order necessary conditions for a minimum are derived by the requirement that the first-order variation of the Lagrangian vanish (this is known as the adjoint method and the resulting conditions are known as the Kuhn–Tucker conditions).

When considering the variation of the structure state equation a linearization is performed,

$$\begin{aligned}\mathbf{G}(D^* + \tilde{D}, W^* + \tilde{W}) = \mathbf{G}(D^*, W^*) &+ \mathbf{G_D}(W^*)\tilde{D} \\ &+ \mathbf{G_W}(D^*)\tilde{W} + h.o.t.,\end{aligned} \tag{3.2}$$

where $\tilde{D}$ and $\tilde{W}$ are small perturbations of the displacement and rigidity from the optimal solution W^* and D^*, respectively, and where the linearized operators $\mathbf{G_D}$ and $\mathbf{G_W}$ are defined as

$$\mathbf{G_D}(W^*)\tilde{D} = \tilde{D}_{xx}W^*_{xx} + \tilde{D}_{yy}W^*_{yy} + \nu[\tilde{D}_{xx}W^*_{yy} + \tilde{D}_{yy}W^*_{xx}] + 2(1-\nu)\tilde{D}_{xy}W^*_{xy} \tag{3.3}$$

$$\mathbf{G_W}(D^*)\tilde{W} = \mathbf{G}(D^*, \tilde{W}).$$

Formally, W^* and D^* serve as nonconstant coefficients in the linearized structure operator.

In the following the costate and design equations are given (on the boundary, $(z = 0)$, $\xi + \lambda = 0$).

Costate equations.

$$\begin{aligned} \overline{\mathbf{L}}\lambda &= 0 \quad z \geq 0 \\ \overline{\mathbf{B}}\lambda - \rho_\infty U_\infty^2 \eta_x &= -F_\phi \quad z = 0 \\ \overline{\mathbf{G}}_\mathbf{W}(D^*)\eta - \lambda_x &= -F_W \quad z = 0. \end{aligned} \tag{3.4}$$

Inflow boundary condition.

Subsonic: $\lambda_x = 0$
Supersonic: No Boundary Condition.

Outflow boundary condition.

Subsonic: $\lambda_x = 0$
Supersonic: $\lambda = 0$ and $\lambda_x = 0$.

Design equations.

$$\begin{aligned} -\lambda_x &= 0 \quad z = 0 \\ \overline{\mathbf{G}}_\mathbf{D}(W^*)\eta + F_D &= 0 \quad z = 0, \end{aligned} \tag{3.5}$$

where

$$\begin{aligned} F_\phi &= -2\gamma_1(\phi_x - f^*)_x - \gamma_3 W_x \\ F_W &= \gamma_3 \phi_x \\ F_D &= \frac{\gamma_2}{d} D^{(1-d)/d}, \end{aligned} \tag{3.6}$$

and where the operators in the adjoint and design equations (3.4–3.5) satisfy

$$\begin{aligned} \overline{\mathbf{L}} &= \mathbf{L} \\ \overline{\mathbf{G}}_\mathbf{W}(D^*) &= \mathbf{G}_\mathbf{W}(D^*) \\ \overline{\mathbf{G}}_\mathbf{D}(W^*) &= \mathbf{G}_\mathbf{D}(W^*). \end{aligned}$$

The adjoint boundary operator $\overline{\mathbf{B}}$ corresponds to the normal derivative, ∂_z, applied to a solution of the interior costate PDE, λ, when using the adjoint far-field boundary conditions. We assume the existence of a solution to the costate equations.

3.2. The Relation of the Hessian with the Necessary Conditions

If the state and costate equations are satisfied then the variation of the Lagrangian (3.1) is equal to the variation in the cost function and is given by

$$\delta\mathcal{L} = \int_\Gamma -\tilde{\alpha}\lambda_x \, d\sigma + \int_\Gamma \tilde{D}(\overline{\mathbf{G}}_\mathbf{D}(W^*)\eta + F_D) \, d\sigma, \tag{3.7}$$

where $\tilde{\alpha}$ and $\tilde{D}$ are variations in the design variables. Therefore, the quantities multiplying $\tilde{\alpha}$ and $\tilde{D}$ in (3.7) are the sensitivity gradients of the cost function with respect to the design variables, when computed on the constraint manifold

$$\begin{aligned} \nabla_\alpha F &= -\lambda_x \\ \nabla_D F &= \overline{\mathbf{G}}_\mathbf{D}(W^*)\eta + F_D. \end{aligned} \tag{3.8}$$

The state and costate equations, (2.1), (2.3), and (3.4), give an implicit relation between the costate variables and the design variables

$$\begin{aligned} \lambda &= \lambda(\alpha, D) \\ \eta &= \eta(\alpha, D). \end{aligned} \tag{3.9}$$

Using Eqs. (3.8) and (3.9) we can write the following relation which holds near the minimum (α^* and D^* denote the optimal value of the design variables α and D, respectively)

$$\begin{aligned} &\nabla_\alpha F(\lambda(\alpha^* + \overline{\alpha}, D^* + \overline{D})) \\ &\qquad = H_{11}\overline{\alpha} + H_{12}\overline{D} + h.o.t. \\ &\nabla_D F(D^* + \overline{D}, \eta(\alpha^* + \overline{\alpha}, D^* + \overline{D})) \\ &\qquad = H_{21}\overline{\alpha} + H_{22}\overline{D} + h.o.t., \end{aligned} \tag{3.10}$$

where at the minimum

$$\nabla_\alpha F(\lambda(\alpha^*, D^*)) = \nabla_D F(D^*, \eta(\alpha^*, D^*)) = 0.$$

We conclude that on the constraint manifold, near the minimum, the Hessian of the cost function relates the errors in the design variables with the residuals of the design equations (sensitivity gradients). In the next section we will use this fact to calculate the symbol of the Hessian.

4. DERIVATION OF THE HESSIAN'S SYMBOL

In the following section we compute the symbol of the Hessian with local mode analysis. Hessian symbols were previously computed for smoothing prediction in the development of multigrid one-shot method [8–11] and lately for

the analysis of inviscid aerodynamic optimization problems [12]. In the following the local mode analysis is outlined.

The analysis is performed in the vicinity of the minimum where the design variables are assumed to have an error $\overline{\alpha}$ and $\overline{D}$. We assume that the state and costate equations are satisfied and consider the errors in the state and costate variables ($\overline{\phi}$, $\overline{W}$, $\overline{\lambda}$, $\overline{\eta}$) with respect to their value at the optimal solution. These errors are assumed to satisfy homogeneous equations similar to Eqs. (2.1, 3.4, 3.5), and a linearization of Eq. (2.3). We then consider the high-frequency errors in the design variables and compute an explicit solution of the problem in terms of exponential functions in a half space. Then with a standard procedure the problem in a half space is reduced to the boundary. On the boundary we study the mapping from the transformed design variables errors to the residuals of the design equations, ($\nabla_\alpha F$, $\nabla_D F$). The symbol of this mapping gives the eigenvalues of the Hessian.

4.1. Fourier Representation

We start with the Fourier representation of the solution in a half space and perform local mode analysis. Consider errors in the solution of the form

$$\begin{aligned}\overline{\alpha}(x,y) &= \hat{\alpha}(\omega_1,\omega_2)e^{i(\omega_1 x+\omega_2 y)}\\ \overline{D}(x,y) &= \hat{D}(\omega_1,\omega_2)e^{i(\omega_1 x+\omega_2 y)}.\end{aligned} \tag{4.1}$$

As a result, the errors in the state and costate variables are assumed to have the form

$$\begin{aligned}\overline{\phi}(x,y,z) &= \hat{\phi}(\omega_1,\omega_2,\omega_3)e^{i(\omega_1 x+\omega_2 y+\omega_3 z)}\\ \overline{\lambda}(x,y,z) &= \hat{\lambda}(\omega_1,\omega_2,\omega_3)e^{i(\omega_1 x+\omega_2 y+\omega_3 z)}\\ \overline{W}(x,y) &= \hat{W}(\omega_1,\omega_2)e^{i(\omega_1 x+\omega_2 y)}\\ \overline{\eta}(x,y) &= \hat{\eta}(\omega_1,\omega_2)e^{i(\omega_1 x+\omega_2 y)}.\end{aligned} \tag{4.2}$$

Before computing the relation between the state and costate error symbols, ($\hat{\phi}$, $\hat{\lambda}$, $\hat{W}$, $\hat{\eta}$), and the design error symbols, ($\hat{\alpha}$, $\hat{D}$), we reduce the problem to the boundary by eliminating ω_3 from the symbols $\hat{\phi}$ and $\hat{\lambda}$.

4.2. Reduction to the Boundary

The reduction to the boundary is done by eliminating ω_3 from the symbol expressions using the interior equations. The following discussion regarding the choice of ω_3 was done in [12] and is repeated here for completeness.

The term $\overline{\phi}$ satisfies the interior equation for ϕ

$$\mathbf{L}\hat{\phi}(\omega_1,\omega_2,\omega_3)e^{i(\omega_1 x+\omega_2 y+\omega_3 z)} = 0. \tag{4.3}$$

Assuming a nontrivial solution, $\hat{\phi} \neq 0$, Eq. (4.3) results in an algebraic relation between ω_1, ω_2, and ω_3

$$(1-M^2)\omega_1^2 + \omega_2^2 + \omega_3^2 = 0. \tag{4.4}$$

The choice of ω_3 should be done such that it will result in a physical solution. We differentiate between subsonic and supersonic flows.

4.2.1. *Subsonic Flow*

In the subsonic regime ($M < 1$) the physical solution is given by

$$\omega_3 = i\sqrt{\omega_1^2(1-M^2)+\omega_2^2},$$

which corresponds to decaying solutions

$$\begin{aligned}\overline{\phi}(x,y,z) &= \hat{\phi}(\omega_1,\omega_2)e^{i(\omega_1 x+\omega_2 y)}e^{-(\sqrt{\omega_1^2(1-M^2)+\omega_2^2})z}\\ \overline{\lambda}(x,y,z) &= \hat{\lambda}(\omega_1,\omega_2)e^{i(\omega_1 x+\omega_2 y)}e^{-(\sqrt{\omega_1^2(1-M^2)+\omega_2^2})z}.\end{aligned}$$

In that case the symbols of the boundary operators, $\mathbf{B}$ and $\overline{\mathbf{B}}$, are given by (recall that $\mathbf{B}$ and $\overline{\mathbf{B}}$ are the normal derivatives applied to a solution of the interior state and costate PDE, respectively)

$$\hat{B} = \hat{\overline{B}} = -\sqrt{\omega_1^2(1-M^2)+\omega_2^2}. \tag{4.5}$$

4.2.2. *Supersonic Flow*

We differentiate between two supersonic cases which are determined by a Mach number denoted M_c and given by

$$M_c = \sqrt{1+\left(\frac{\omega_2}{\omega_1}\right)^2}.$$

The case $1 \le M \le M_c$ results in the same symbols for $\hat{B}$ and $\hat{\overline{B}}$ as for the subsonic flow case (Eq. (4.5)).

In the case $M_c < M$ both signs of ω_3 in (4.4) correspond to physical solutions. The positive root correspond to the characteristic which propagates into the shape, ϕ_+, and the negative root correspond to the characteristic which propagates out of the shape, ϕ_-, (and a similar expression of λ)

$$\begin{aligned}\overline{\phi}(x,y,z) = {}& \hat{\phi}_+(\omega_1,\omega_2)e^{i(\omega_1 x+\omega_2 y+\sqrt{|\omega_1^2(1-M^2)+\omega_2^2|}z)}\\ &+ \hat{\phi}_-(\omega_1,\omega_2)e^{i(\omega_1 x+\omega_2 y-\sqrt{|\omega_1^2(1-M^2)+\omega_2^2|}z)}.\end{aligned} \tag{4.6}$$

Since the inflow information does not change as a result of a shape perturbation, the following holds:

$$\overline{\phi}_+(x,y,z) = 0. \tag{4.7}$$

In the same manner the outflow characteristic of the adjoint is not changing as a result of a shape perturbation:

$$\overline{\lambda}_{-}(x, y, z) = 0. \tag{4.8}$$

Therefore,

$$\overline{\phi}(x, y, z) = \hat{\phi}_{-}(\omega_1, \omega_2) e^{i(\omega_1 x + \omega_2 y - \sqrt{|\omega_1^2(1-M^2)+\omega_2^2|}z)}$$
$$\overline{\lambda}(x, y, z) = \hat{\lambda}_{+}(\omega_1, \omega_2) e^{i(\omega_1 x + \omega_2 y + \sqrt{|\omega_1^2(1-M^2)+\omega_2^2|}z)}$$

We conclude that for flow speeds $M_c < M$ the boundary operator $\mathbf{B}$ is antisymmetric, (with respect to the adjoint operation), and the symbols $\hat{B}$ and $\hat{\overline{B}}$ are given by

$$\begin{aligned} \hat{B} &= -i\sqrt{|\omega_1^2(1-M^2)+\omega_2^2|} \\ \hat{\overline{B}} &= i\sqrt{|\omega_1^2(1-M^2)+\omega_2^2|}. \end{aligned} \tag{4.9}$$

In all flow conditions the multiplication $\hat{B}\hat{\overline{B}}$ results in the same expression:

$$\hat{B}\hat{\overline{B}} = |\omega_1^2(1-M^2)+\omega_2^2|. \tag{4.10}$$

By eliminating ω_3 from the transformed equations the state and costate flow equations can be written on the surface (ω_1, ω_2) which corresponds to the boundary (x, y).

4.3. Treatment of the Structure Equations

In this subsection we give a short note concerning the transformation of the structure state and costate equations. The structure state and costate equations contain nonconstant coefficients which should be frozen prior to the local mode analysis. The structure state and costate error equations are given by (see Eqs. (2.3, 3.2, 3.4))

$$\begin{aligned} \mathbf{G_D}(W^*)\overline{D} + \mathbf{G_W}(D^*)\overline{W} &= \rho_\infty U_\infty^2 \overline{\phi}_x \quad z = 0 \\ \overline{\mathbf{G}}_{\mathbf{W}}(D^*)\overline{\eta} - \overline{\lambda}_x &= -\overline{F}_W \quad z = 0, \end{aligned} \tag{4.11}$$

where $\overline{D}$, $\overline{W}$, $\overline{\phi}$, $\overline{\eta}$, and $\overline{\lambda}$ denote the error variables, $\overline{F}_W$ denotes the error in F_W, and the operators $\mathbf{G_D}$ and $\mathbf{G_W}$ are defined in (3.3). Since Eqs. (4.11) have variable coefficients, D^* and W^*, it is necessary to freeze them around a point on the boundary. This procedure is justified as long as the errors in the design variables are highly oscillatory compared to W^* and D^*. We denote the values of $W^*(x, y)$ and $D^*(x, y)$ at a point (x_0, y_0) on the boundary by W_0^* and D_0^*, respectively.

4.4. The Coupled State and Costate Equations in Fourier Space

In terms of their Fourier representation on the boundary, the state and costate error equations are given by the matrix form

$$\begin{pmatrix} \hat{B} & -i\omega_1 & 0 & 0 \\ -\rho_\infty U_\infty^2 i\omega_1 & \hat{G}_W(D_0^*) & 0 & 0 \\ -\hat{F}_{\phi\phi} & -\hat{F}_{\phi W} & \hat{\overline{B}} & -\rho_\infty U_\infty^2 i\omega_1 \\ \hat{F}_{W\phi} & 0 & -i\omega_1 & \hat{\overline{G}}_W(D_0^*) \end{pmatrix} \begin{pmatrix} \hat{\phi} \\ \hat{W} \\ \hat{\lambda} \\ \hat{\eta} \end{pmatrix} = \begin{pmatrix} i\omega_1\hat{\alpha} \\ -\hat{G}_D(W_0^*)\hat{D} \\ 0 \\ 0 \end{pmatrix}. \tag{4.12}$$

The various symbols are given explicitly by

$$\begin{aligned} \hat{F}_{\phi\phi} &= 2\gamma_1\omega_1^2 \\ \hat{F}_{\phi W} &= -i\gamma_3\omega_1 \\ \hat{F}_{W\phi} &= i\gamma_3\omega_1 \\ \hat{G}_W(D_0^*) &= D_0^*(\omega_1^2+\omega_2^2)^2 + l.o.t. \\ \hat{G}_D(W_0^*) &= -\omega_1^2(W_{0xx}^* + \nu W_{0yy}^*) - \omega_2^2(W_{0yy}^* + \nu W_{0xx}^*) \\ &\quad - \omega_1\omega_2(2(1-\nu)W_{0xy}^*). \end{aligned} \tag{4.13}$$

Note that the terms originating in the cost function serve as a coupling symmetric block between the state and costate systems.

4.5. The Symbol of the Hessian

The design equations residuals, in the transformed space, are given by

$$\begin{aligned} \hat{g}_1 &= -i\omega_1\hat{\lambda} \\ \hat{g}_2 &= \hat{\overline{G}}_D(W_0^*)\hat{\eta} + \hat{F}_{DD}(D_0^*)\hat{D}, \end{aligned} \tag{4.14}$$

where $\hat{F}_{DD}$ is the linearization of F_D in (3.6),

$$\hat{F}_{DD} = \frac{\gamma^2(1-d)}{d^2}(D_0^*)^{(1-2d)/d},$$

and the symbols $\hat{g}_1$ and $\hat{g}_2$ are the symbols of the sensitivity gradients $\nabla_\alpha F$ and $\nabla_D F$, respectively (see (3.8)).

Inverting the system (4.12) and substituting $\hat{\lambda}$ and $\hat{\eta}$ in the symbol of the design residuals (4.14) results in a relation between the residuals of the design equations and the errors in the design variables. In Fourier space,

$$\begin{pmatrix} \hat{g}_1 \\ \hat{g}_2 \end{pmatrix} = \begin{pmatrix} \hat{H}_{11} & \hat{H}_{12} \\ \hat{H}_{21} & \hat{H}_{22} \end{pmatrix} \begin{pmatrix} \hat{\alpha} \\ \hat{D} \end{pmatrix}, \tag{4.15}$$

where the matrix $\hat{H}_{ij}$ is the symbol of the Hessian, as discussed in Sec. 3.2. $\hat{H}_{11}$ is the symbol of the aerodynamic optimization Hessian, $\hat{H}_{22}$ of the structural optimization Hessian, and $\hat{H}_{12}, \hat{H}_{21}$ are the coupling terms. In the following, the terms $\hat{H}_{ij}$ are given explicitly

$$\hat{H}_{11} = \frac{\omega_1^2 \hat{G}_W}{\widehat{\det}} (\hat{F}_{\phi\phi} \hat{G}_W + 2\rho_\infty U_\infty^2 i\omega_1 \hat{F}_{\phi W}) \tag{4.16}$$

$$\hat{H}_{12} = \frac{i\omega_1 \hat{G}_D}{\widehat{\det}} (i\omega_1 \hat{F}_{\phi\phi} \hat{G}_W + \hat{B} \hat{F}_{\phi W} \hat{G}_W - \rho_\infty U_\infty^2 \omega_1^2 \hat{F}_{\phi W}) \tag{4.17}$$

$$\hat{H}_{21} = \frac{i\omega_1 \hat{G}_D}{\widehat{\det}} (i\omega_1 \hat{F}_{\phi\phi} \hat{G}_W + \hat{\bar{B}} \hat{F}_{\phi W} \hat{G}_W - \rho_\infty U_\infty^2 \omega_1^2 \hat{F}_{\phi W}) \tag{4.18}$$

$$\hat{H}_{22} = -\frac{i\omega_1 \hat{G}_D^2}{\widehat{\det}} (i\omega_1 \hat{F}_{\phi\phi} + (\hat{B} + \hat{\bar{B}}) \hat{F}_{\phi W}) + \hat{F}_{DD}, \tag{4.19}$$

where $\widehat{\det}$ is the determinant symbol given by

$$\widehat{\det} = (\hat{B} \hat{G}_W + \omega_1^2 \rho_\infty U_\infty^2)(\hat{\bar{B}} \hat{G}_W + \omega_1^2 \rho_\infty U_\infty^2). \tag{4.20}$$

Since $\hat{G}_W$ is a fourth order polynomial in $\omega_{1,2}$, $\hat{G}_D$, $\hat{F}_{\phi\phi}$, $\hat{B}$, and $\hat{\bar{B}}$ are of second order, $\hat{F}_{\phi W}$ is first order, and $\hat{F}_D$ is of zero order, the principal parts of the above expressions (the asymptotic limits of high frequencies), are given by

$$\hat{H}_{11} \approx \frac{\omega_1^2 F_{\phi\phi}}{\hat{B}\hat{\bar{B}}} = 2\gamma_1 U_\infty^2 \frac{\omega_1^4}{|\omega_1^2(1 - M^2) + \omega_2^2|} \tag{4.21}$$

$$\hat{H}_{12} = \hat{H}_{21} \approx \frac{-\omega_1^2 \hat{G}_D \hat{F}_{\phi\phi}}{\hat{B}\hat{\bar{B}} \hat{G}_W} = \frac{2\gamma_1 U_\infty^2 \omega_1^4}{D_0^*} \cdot \left[\frac{\omega_1^2 (W_{0xx}^* + \nu W_{0yy}^*)}{|\omega_1^2(1 - M^2) + \omega_2^2| \cdot (\omega_1^2 + \omega_2^2)^2} + \frac{\omega_2^2 (W_{0yy}^* + \nu W_{0xx}^*) + 2\omega_1\omega_2(1 - \nu) W_{0xy}^*}{|\omega_1^2(1 - M^2) + \omega_2^2| \cdot (\omega_1^2 + \omega_2^2)^2} \right] \tag{4.22}$$

$$\hat{H}_{22} \approx \hat{F}_{DD} = \frac{\gamma_2 (1 - d)}{d^2} (D_0^*)^{(1-2d)/d}. \tag{4.23}$$

Note that for simplicity we assumed a complex representation of the errors, (4.1), and obtained a complex Hessian symbol. If considering a real representation, i.e.,

$$\overline{\alpha}(x, y) = \hat{\alpha}(\omega_1, \omega_2) e^{i(\omega_1 x + \omega_2 y)} + \hat{\alpha}^{conj}(\omega_1, \omega_2) e^{-i(\omega_1 x + \omega_2 y)},$$

where $\hat{\alpha}^{conj}$ is the complex conjugate of $\hat{\alpha}$, and a similar expression for $\overline{D}$, then the resulting Hessian symbol is real and symmetric.

4.6. Discretization and the Condition Number

In practice the problem is solved numerically and thus discretization is introduced. Therefore the analysis should be performed in the discrete space and the Hessian will depend on the specific discretization. For the "ideal" discretization, the symbol of the Hessian is equal to the differential one with the substitution

$$(\omega_1, \omega_2) = \left(\frac{\theta_1}{h_1}, \frac{\theta_2}{h_2} \right),$$

where (h_1, h_2) are the mesh sizes in the (x, y) directions, respectively, and where θ_1 and θ_2 vary in the domain $[-\pi, \pi]$.

Note that "high frequencies" are those which obey $\omega_i \geqslant c$ for some constant, c, which is determined by the different parameters in the problem. In the discrete space this corresponds to $\theta_i \geqslant c h_i$. Since the constant c is independent of the mesh size h, as the grid is refined the portion of high frequencies in the spectrum increases and therefore the approximation taken by the local mode analysis above is more accurate for a larger part of the spectrum. This is not surprising since as the grid is refined its resolution increases while the resolution of the smooth components remains unchanged.

The maximum eigenvalue of each of the disciplinary Hessians is estimated by

$$\lambda_{max} = \hat{H}_{ii} \left(\frac{\pi}{h} \right).$$

Unfortunately, the lowest eigenvalue cannot be estimated by the procedure above since this is precisely the spectrum range in which the approximation taken by the local mode analysis does not hold. Still, it is reasonable to assume that the lowest eigenvalue is asymptotically a fixed number as the mesh refines and therefore the condition number of the Hessian is proportional to λ_{max}. For a two-dimensional flow over a beam, ($\omega_2 = 0$), we get for the aerodynamic part of the Hessian (see Eq. (4.21))

$$\lambda_{max} = \frac{2\gamma_1 U_\infty^2 \pi^2}{|1 - M^2|} \frac{1}{h^2}.$$

We conclude that the aerodynamic part of the Hessian is ill conditioned and its condition number is increasing as the grid is refined (see [12] for further discussion). The

structure's symbol (4.23) approaches a constant, for the high frequencies, independent of the mesh size. We therefore conclude that the structural optimization problem is well conditioned.

5. APPLICATIONS TO OPTIMIZATION STRATEGIES

In the previous section we computed explicitly the Hessian's symbol. In this section we discuss the applications of this result to optimization strategies for the solution of the aeroelastic optimization problem. We differentiate between two basic approaches, the ''disciplinary'' and the ''multidisciplinary.'' In the disciplinary approach the solution of the problem is divided so that one discipline optimization problem is solved at each stage, decoupled from the other discipline. In the multidisciplinary approach both the analysis and optimization solutions are performed in a tightly coupled manner. These two approaches are now presented in more detail.

5.1. The Multidisciplinary Approach—Tight Coupling

Lately there has been an effort to develop new optimization strategies which couple the two disciplines tightly during the analysis and optimization computation. This is known as the MDO approach [1–7]. According to this approach after each call to the optimizer the analysis and adjoint equations are relaxed, or solved exactly, depending on the feasibility choice (Multidisciplinary Feasibility (MDF), Individual Discipline Feasibility (IDF) or All at Once (AAO), [3]).

The MDO Algorithm.

The coupled aerodynamic shape and structure minimum weight optimization problems are solved simultaneously:

$$\min_{\alpha,D} \gamma_1 \int_\Gamma (\phi_x - f^*)^2 \, dx + \gamma_2 \int_\Gamma D^{1/d} \, dx + \gamma_3 \int_\Gamma pW \, dx$$

subject to

$$L\phi = 0 \quad z \geq 0$$

$$B\phi = (\alpha_x + W_x) \quad z = 0$$

$$G(D, W) = -p \quad z = 0$$

where the pressure is given by $p = (p_\infty - \rho_\infty U_\infty^2 \phi_x)$.

5.2. The Disciplinary Approach—Weak Coupling

A common practical strategy used to solve large aeroelastic shape optimization problems is the disciplinary approach; i.e., design the aerodynamic optimal shape to give the best performance and then design a minimum weight structure, restricted to the aerodynamic shape. The costate η (λ) is used in the aerodynamic (structural) design to account for the term

$$\frac{\partial F}{\partial W}\frac{\partial W}{\partial \phi}\frac{\partial \phi}{\partial \alpha}\left(\frac{\partial F}{\partial \phi}\frac{\partial \phi}{\partial W}\frac{\partial W}{\partial D}\right)$$

(in many applications this term is constructed by sensitivity analysis rather than by the adjoint method as done in this paper).

The Disciplinary Algorithm.

1. The aerodynamic shape optimization problem is solved given a fixed rigidity D, deflection W, and structure costate η:

$$\min_\alpha \int_\Gamma (\phi_x - f^*)^2 \, d\sigma$$

subject to

$$L\phi = 0 \quad z \geq 0$$

$$B\phi = \alpha_x + W_x \quad z = 0.$$

2. The structure minimum weight problem is solved given a fixed aerodynamic shape α, potential ϕ, and aerodynamic costate λ:

$$\min_D \gamma_2 \int_\Gamma D^{1/d} \, d\sigma + \gamma_3 \int_\Gamma pW \, d\sigma$$

subject to

$$G(D, W) = -p \quad z = 0.$$

3. If some convergence criteria is met then stop, otherwise go to 1.

We define a ''disciplinary iteration'' as one application of steps 1 and 2 in the above algorithm (the order being interchanged, i.e., apply first step 2 followed by step 1). We say that the optimization problem is *loosely coupled* if one disciplinary iteration results in a significant error reduction in all the design variables. In that case the disciplinary algorithm should converge to the multidisciplinary optimal solution with a small number of disciplinary iterations. In a two discipline system we claim that the system is loosely coupled if in one of the rows in the Hessian's symbol there is a diagonal dominant term. In that case the set of design variables that correspond to the dominant term can be determined, to a good approximation, while

freezing the other variables, thus the problem is loosely coupled. In the following subsections we simplify the result (4.21)–(4.23) for two and three space dimensions and show that in both cases the Hessian's symbol is diagonal dominant in the first row (corresponding to the aerodynamic part) indicating loose coupling in the MDO problem.

5.3. Two Space Dimensions

In a two-dimensional flow over a beam the principal part of the Hessian is given by (see Eqs. (4.21)–(4.23))

$$\hat{H}(\omega_1 \gg 1) = 2\begin{pmatrix} \dfrac{\gamma_1 U_\infty^2}{|1-M^2|}\omega_1^2 & \dfrac{\gamma_1 U_\infty^2}{|1-M^2|}\dfrac{W^*_{0xx}}{D^*_0} \\ \dfrac{\gamma_1 U_\infty^2}{|1-M^2|}\dfrac{W^*_{0xx}}{D^*_0} & -\dfrac{1}{8}\gamma_2 D_0^{*-3/2} \end{pmatrix}. \quad (5.1)$$

The matrix (5.1) implies that for the nonsmooth error components in the design variables

$$\hat{H}_{11} \geq H_{12}. \quad (5.2)$$

Assuming that the errors in the structural design variables are of the same order of magnitude as the errors in the shape design variables,

$$\overline{D} \approx \overline{\alpha} \quad (5.3)$$

we conclude that the equation

$$H_{11}\overline{\alpha} + H_{22}\overline{D} = -g_1 \quad (5.4)$$

can be approximated by the equation

$$H_{11}\tilde{\alpha} = -g_1. \quad (5.5)$$

As a result the error in the aerodynamic design variable, $\overline{\alpha}$, is not sensitive to the error in the rigidity, $\overline{D}$, and therefore can be computed to a good approximation independently.

5.4. Three Space Dimensions

In a three-dimensional configuration we differentiate between the stream-wise and span-wise directions. Let us assume that the curvature of the deflection in the stream-wise direction is negligible; i.e., set $W^*_{0xx} = 0$. As a result the coupling term $\hat{H}_{12}$ has the form

$$\hat{H}_{12}(W^*_{0xx} = 0) \approx \frac{2\gamma_1 U_\infty^2}{D_0^*}\frac{\omega_1^4(\omega_1^2 \nu W^*_{0yy} + \omega_2^2 W^*_{0yy} + 2\omega_1\omega_2(1-\nu)W^*_{0xy})}{|\omega_1^2(1-M^2) + \omega_2^2| \cdot (\omega_1^2 + \omega_2^2)^2}. \quad (5.6)$$

For the design of the structure in the span-wise direction only, i.e., freezing the stream-wise design as done in practice for aircraft wing design, the off-diagonal terms in the Hessian vanish, ($\omega_1 = 0$), and therefore the problem is decoupled.

For errors in the stream-wise direction only, (i.e., $\omega_2 = 0$), the off-diagonal terms in the Hessian reduce to

$$\hat{H}_{12}(\omega_2 = 0) \approx \frac{2\gamma_1 U_\infty^2 \nu W^*_{0yy}}{D_0^*|1-M^2|}.$$

By a similar argument as done for the two-dimensional case the three-dimensional optimization problem is also loosely coupled.

6. NUMERICAL TESTS

In the numerical test we considered a two-dimensional potential flow over a one-dimensional beam. The problem was to compute the set $\{D_i^h\}_{i=1}^N$ and the set $\{\alpha_i^h\}_{i=1}^N$ such that the following cost functional is minimized (we denote the discrete quantities by a superscript h),

$$F(\phi, W, D) = \gamma_1 \sum_{i=1}^N ((\phi_x^h)_i - f_i^{*h})^2 + \gamma_2 \sum_{i=1}^N (D_i^h)^{1/2} + \gamma_3 \sum_{i=1}^N (\phi_x^h)_i W_i^h + \frac{1}{2}\gamma_4 \sum_{i=1}^N (\alpha_i^h)^2 \quad (6.7)$$

subject to the inequality constraint

$$D_i^h \geq D_{min} \quad 1 < i < N \quad (6.8)$$

and to the following finite difference equations,

$$\begin{aligned} (1-M_\infty^2)\partial_{xx}^h \phi_{i,k}^h + \partial_{zz}^h \phi_{i,k}^h &= 0 && 1 < i, k < N \\ \partial_z^h \phi_{i,1}^h &= \partial_x^h(\alpha_i^h + W_i^h) && 1 < i < N \\ \phi_{1,k}^h &= \phi_{2,k}^h && 1 < k < N \\ \phi_{N,k}^h &= \phi_{N-1,k}^h && 1 < k < N \\ \phi_{i,N}^h &= 0 && 1 < i < N \end{aligned} \quad (6.9)$$

$$\begin{aligned}
&\partial^h_{xx}(D^h_i \partial^h_{xx} W^h_i) = -p^h_i \qquad 1 < i < N \\
&W^h_1 = W^h_N = 0 \\
&\partial^h_x W^h_1 = \partial^h_x W^h_N = 0 \qquad \text{for a clamped beam} \\
&\partial^h_{xx} W^h_1 = \partial^h_{xx} W^h_N = 0 \qquad \text{for a simply supported beam,}
\end{aligned} \tag{6.10}$$

where ∂^h_x, ∂^h_z, ∂^h_{xx} and ∂^h_{zz} denote finite difference operators for the first and second derivatives in the x and z directions, respectively.

In the numerical test the far field parameters were set to unity except the far field Mach number which was set to 0.5

$$p_\infty = \rho_\infty = U_\infty = 1;\ M_\infty = 0.5.$$

The fourth term in the cost function was added for uniqueness of the optimal solution α^* (since only the derivative α_x appears in the equations). The weights in the cost functional were determined to establish significant coupling between the disciplines, in particular that at the optimal solution the deflection, W^*, and the shape, α^*, have the same order of magnitude (see Figs. 1b (2b) and 1c (2c)):

$$\gamma_1 = \gamma_3 = \gamma_4 = 1;\ \gamma_2 = 0.01.$$

In order to avoid singularities in the beam equation, $D^h = 0$, an inequality constraint has been applied on the rigidity

$$D(x) \geq D_{min}(x) \quad 0 \leq x \leq 1, \tag{6.11}$$

where the minimal value of the rigidity was set to $D_{min}(x) = 10^{-4}$ (in the case of a clamped beam this constraint was binding for two design variables as depicted in Fig. 2d).

The computational grid consisted of an $(N \times N)$ grid on which the potential equation was solved in the whole domain while the beam equation was solved on the boundary ($z = 0$). On each grid on the boundary, $1 \leq i \leq N$, two design variables were defined: α^h_i and D^h_i.

6.1. Derivation of the Gradient

The gradient of the cost functional (6.7) with respect to the $2N$ design variables, $\{D\}^N_{i=1}$ and $\{\alpha\}^N_{i=1}$, was derived with the discrete adjoint method. A Lagrangian was defined in the discrete level, similar to the continuum level (see Eq. (3.1)), as the sum of the discrete cost functional and discrete costate variables multiplying the residuals of the state finite difference equations. The variation of the Lagrangian with respect to the state variables resulted in finite difference equations for the costate variables. The variation of the Lagrangian with respect to the design variables resulted in the cost functional gradients.

6.2. Numerical Results

Two numerical cases were considered: a simply supported beam which has zero moment at the boundaries ($W = W_{xx} = 0$) and a clamped beam which has zero change in the deflection at the boundaries ($W = W_x = 0$). In the two cases a tightly coupled solution was achieved with the MDO algorithm (see Section 5.1). The cost functional (6.7) was driven to a local minimum at which the gradients vanished. We denote that solution by (α^*, D^*).

In a second stage, the disciplinary solution (see Section 5.2) was obtained by the following steps. We started from an initial guess for the design variables (α_0, D_0) and solved the state and costate equations for this initial guess. Then the structural optimization problem was solved keeping the aerodynamic variables, $\{\alpha^h_i,\ \phi^h_{i,j},\ \lambda^h_{i,j}\}^N_{i,j=1}$, fixed (as explained in Section 5.2). The optimal rigidity solution at this stage was denoted by D_1. Then the state and costate equations were solved on (α_0, D_1) and the aerodynamic optimization problem was solved while keeping the structure variables, $\{D^h_i, W^h_i, \eta^h_i\}^N_{i=1}$, fixed. The optimal aerodynamic shape solution at this stage was denoted by α_1. This procedure was repeated a second time for D_2 and α_2.

The results ($N = 8$) for the simply supported and clamped cases are depicted in Figs. 1 and 2, respectively. Figure 1a (2a) depicts the tangential derivative of the potential at the optimal solution versus the target distribution f^*. Figure 1b (2b) depicts the deflection at the optimal solution. Figure 1c (2c) depicts the aerodynamic design variables $\{\alpha_i\}^N_{i=1}$ at different stages of the disciplinary solution: α^* is the solution of the tightly coupled (multidisciplinary) algorithm, α_0 is the initial design, α_1 is the solution after a single disciplinary iteration, and α_2 is the solution after two disciplinary iterations. Figure 1d (2d) depicts the result for the structural design variables $\{D_i\}^N_{i=1}$. As predicted by the local mode analysis the disciplinary algorithm converges to the MDO solution very effectively. It took practically two disciplinary iterations to recover the MDO solution.

7. CONCLUDING REMARKS

The symbol of the Hessian for a static aeroelastic optimization model problem was computed for the nonsmooth error components in the design variables (Eqs. (4.16)–(4.19)). The result indicates that for the nonsmooth components the multidisciplinary optimization system can be decoupled to the single discipline optimization problems. Such a sequential approach should converge to the multidisciplinary solution with a small number of disciplinary iterations. The result also indicates that the aerodynamic

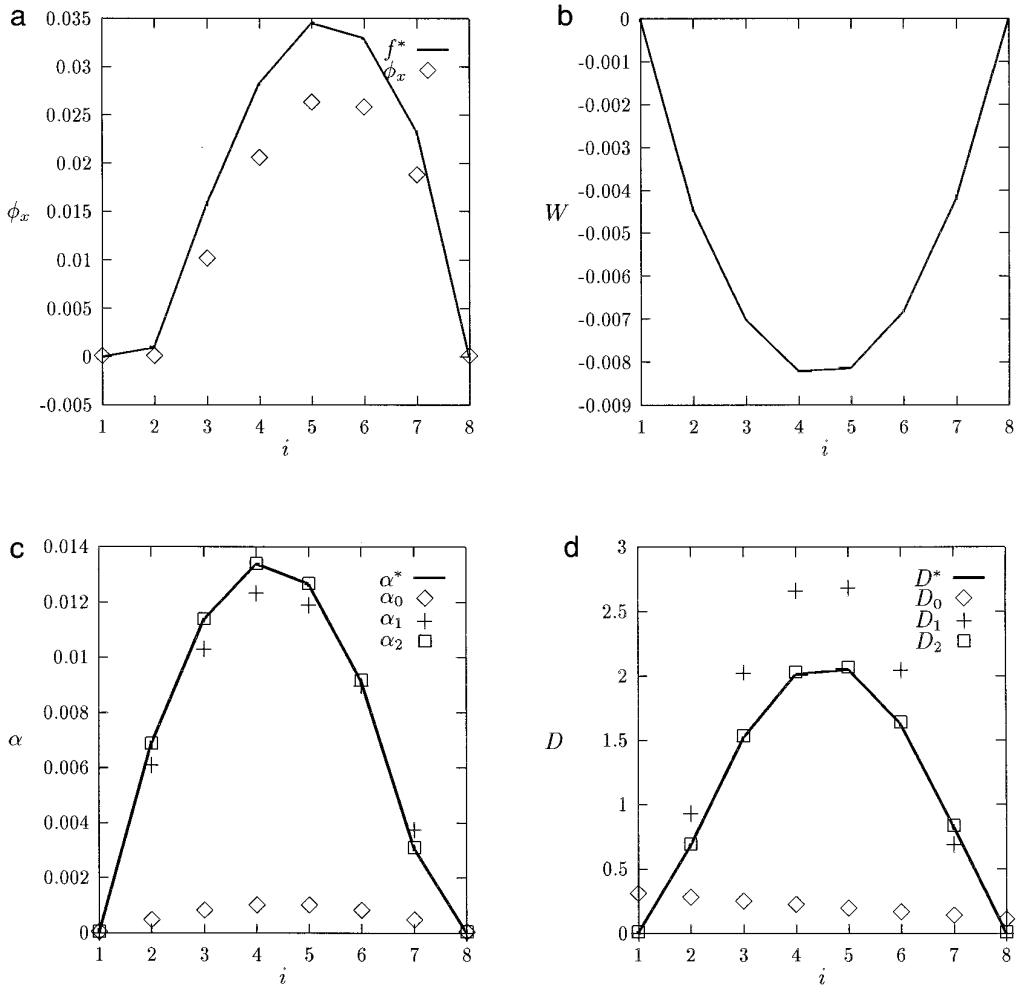

FIG. 1. Simply supported case: (a) the tangential derivative of the potential at the optimal solution versus the target distribution f^*; (b) the deflection at the optimal solution; (c) the aerodynamic shape at different stages of the disciplinary algorithm. Starting from an initial guess α_0, after one iteration of the disciplinary algorithm the solution α_1 was obtained. The MDO solution is given by α^*. Panel (d) depicts the results for the rigidity similarly to the shape in (c).

optimization problem is ill conditioned, and therefore second order information is essential for efficiently solving this part of the problem [12], while the structural optimization problem is well conditioned. Thus, it is anticipated that the number of optimization iterations required to solve the multidisciplinary problem is determined by the aerodynamic optimization part of the problem.

The aim of the MDO approach is to couple a refined CFD code with a detailed finite-element structural analysis code to compute the aeroelastic states prior to each optimization iteration. The computational complexity of the MDO algorithm is much greater than that of the disciplinary algorithm since at each multidisciplinary iteration both the aerodynamic and structural optimization problems have to be solved. Moreover, the MDO problem can be ill conditioned even when each of the disciplinary optimization problem is well conditioned (the MDO approach also introduces a technical difficulty of joining together two large codes). The results shown in this paper indicate that the MDO approach applied on a fine scale model might not be necessary to obtain a good approximation of the optimal solution. The effect of the smooth components can be captured by a coarse model containing a relatively small number of design variables and thus can be solved by the MDO approach with a relatively low computational cost. This will require simple models for the flow (panel method or small disturbance potential on a coarse grid) coupled with a plate model, or coarse finite-element model, for the structure.

If indeed for a given static aeroelastic optimization problem the aerodynamic block in the Hessian (H_{11}) is

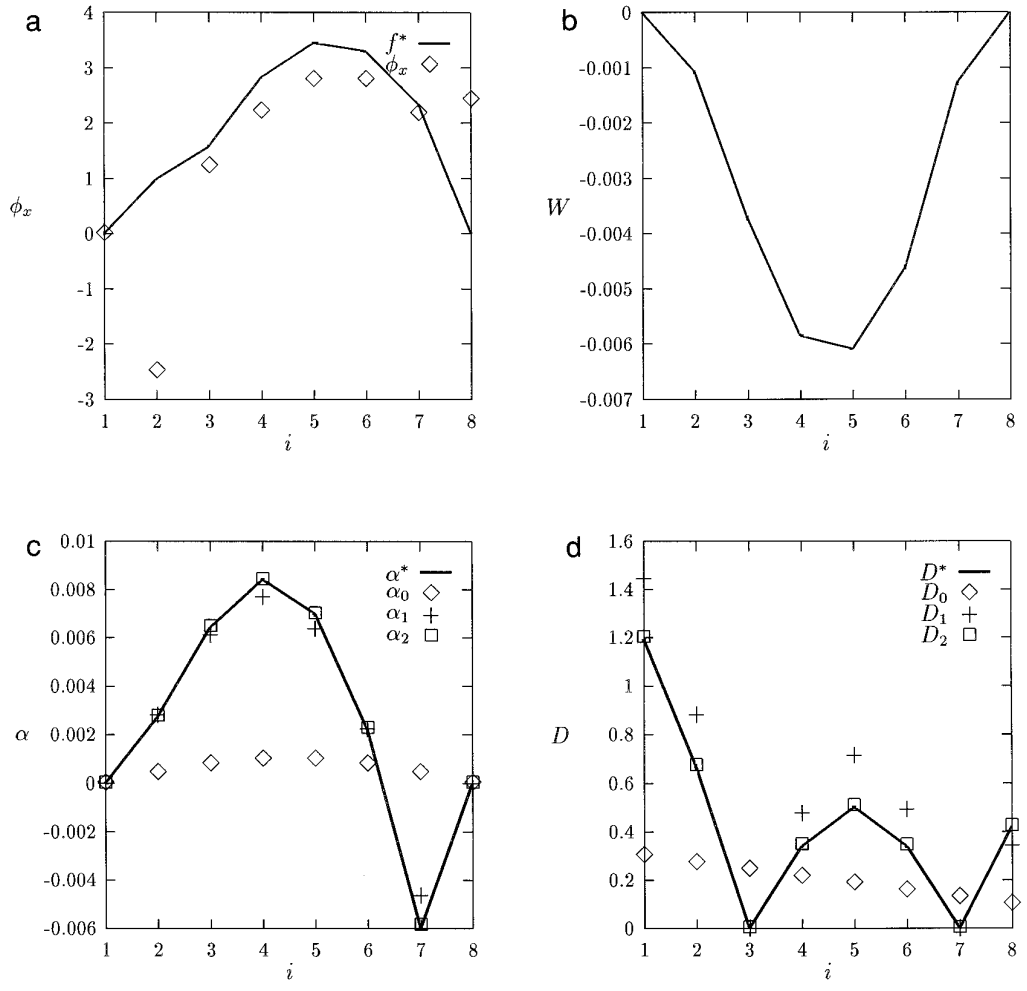

FIG. 2. Clamped case: Panels (a–d) are as described in the legend for Fig. 1(a–d). Note that in this case the rigidity tends to zero at two points ($i = 3$ and $i = 7$). At these points the constraint is binding and $D_i = 10^{-4}$.

dominant over the coupling block (H_{12}) for the non-smooth components, as discussed, we propose that such problems be solved in two stages as illustrated in Fig. 3. In the first stage, the MDO approach will be applied on a coarse model. The second stage starts with the solution of the MDO algorithm and the refined problem is solved with the disciplinary algorithm, thus avoiding the enormous complexity of the MDO algorithm when applied on the fine scale model. We claim that the resulting design will be a good approximation of the optimal solution. We emphasize that this is possible due to the loose coupling between the two discipline design problems, otherwise the proposed approach will require numerous disciplinary iterations and therefore in that case the MDO approach should be applied also on fine scales.

A numerical test has been done for the model problem presented in the paper. The numerical test clearly supports the predictions of the analysis: within two disciplinary iterations the multidisciplinary solution has been recovered.

Finally, how far can we extrapolate the conclusions from this model problem to a more realistic model?

As for the aerodynamic model, it is shown in [12] that an identical symbol for the aerodynamic part of the Hessian is obtained when using Euler equations instead of the full potential. The analysis for the Navier–Stokes equations has not yet been completed. Shocks were also neglected in the aerodynamic model, but we postulate that they are not going to change the main conclusion since shocks have a global effect and are not likely to affect the conditioning of the Hessian.

As for the specific modeling which we have chosen to analyze, since there are many different models for the cost function and different constraints depending on the application, it is impractical to analyze them all.

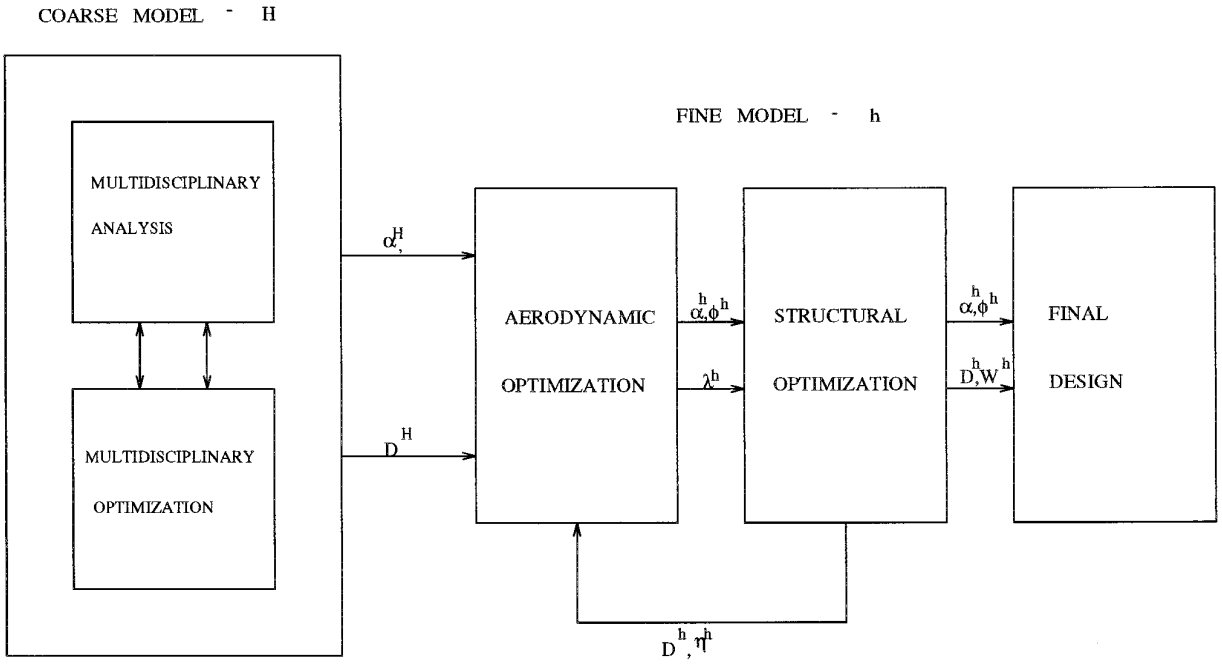

FIG. 3. An optimization strategy to solve aeroelastic optimization problems in case of *loose coupling* as defined in Section 5. Apply the MDO approach on a coarse model followed by a disciplinary serial approach on fine scales. The result should be a good approximation of the multidisciplinary optimal solution.

Changes in the shape were considered in the normal direction only (the planform remains fixed) and therefore no conclusions are made as to the coupling between the aerodynamic and the structural design when the planform's shape is allowed to change during the optimization.

ACKNOWLEDGMENTS

This research was supported by the National Aeronautics and Space Administration under NASA Contract No. NAS1-19480. The author thanks R. T. Haftka, J. W. Hou, and J. A. Burns for fruitful discussions during different stages of this work.

REFERENCES

1. J. S. Sobieszczanski-Sobieski, *AIAA J.* **28**(1), (1990).
2. *5th AIAA/USAF/NASA/SSMO Symposium on Multidisciplinary Analysis and Optimization, Panama City, Florida, Sept. 7–9, 1994.*
3. E. J. Cramer, J. E. Dennis, Jr., P. D. Frank, R. M. Lewis, and G. R. Shubin, *SIAM J. Opt.* ***4***(4), 754 (1994).
4. N. Alexandrov and M. Y. Hussaini, Multidisciplinary design optimization state-of-the-art, *SIAM Proceedings in Applied Mathematics 80, Workshop held in Hampton, Virginia, Mar. 1995.*
5. G. R. Shubin, *J. Comput. Phys.* **118,** (1995).
6. A. E. Arslan and L. A. Carlson, Integrated determination of sensitivity derivatives for an aeroelastic transonic wing, AIAA-94-4400-CP, pp. 1286–1300, in *5th AIAA/USAF/NASA/SSMO Symposium on Multidisciplinary Analysis and Optimization, Panama City, Florida, Sept. 7–9, 1994.*
7. C. J. Borland, J. R. Benton, P. D. Frank, T. J. Kao, R. A. Mastro, and J-F. M. Barthelemy, Multidisciplinary design optimization of a commercial aircraft wing—An exploratory study, AIAA-94-4305-CP, pp. 505–519, in *5th AIAA/USAF/NASA/SSMO Symposium on Multidisciplinary Analysis and Optimization, Panama City, Florida, Sept. 7–9, 1994.*
8. E. Arian, *Multigrid Methods for Optimal Shape Design Governed by Elliptic Systems,* Ph.D. thesis, The Weizmann Institute of Science, Israel, 1994.
9. E. Arian and S. Ta'asan, *Multigrid One Shot Methods for Optimal Design Problems: Infinite-Dimensional Control,* ICASE Report No. 94-52 (1994).
10. E. Arian, and S. Ta'asan, *Shape Optimization in One Shot, Optimal Design and Control,* edited by J. Boggaard, J. Burkardt, M. Gunzburger, and J. Peterson, (Birkhäuser, Boston, 1995).
11. E. Arian, S. Ta'asan, Smoothers for Optimization Problems, *Seventh Copper Mountain Conference on Multigrid Methods,* Apr. 2–7, 1995.
12. E. Arian and S. Ta'asan, *Analysis of the Hessian for Aerodynamics Optimization: Inviscid Flow,* ICASE Report No. 96-28 (1996).
13. W. P. Huffman, R. G. Melvin, D. P. Young, F. T. Johnson, J. E. Bussoletti, M. B. Bieterman, and C. L. Hilmes (The Boeing Company), Practical design and optimization in computational fluid dynamics, AIAA 93-3111, in *Fluid Dynamics Conference, July 6–9, 1993.*
14. S. Timoshenko and S. Woinowsky-Krieger, *Theory of Plates and Shells,* Second Edition, McGraw-Hill, New York, 1970.
15. E. H. Dowell, *Aeroelasticity of Plates and Shells,* Noordhoff, Leyden, 1975.
16. M. J. Lighthill, A new method of two dimensional aerodynamic design. R&M 1111, Aeronautical Research Council, 1945.

17. A. Jameson, *J. Sci. Comput.* **3,** (1988).

18. S. Ta'asan, G. Kuruvila, and M. D. Salas, Aerodynamic design and optimization in one shot, in *30th Aerospace Sciences Meeting & Exhibit, AIAA 92-0025, Jan.* 1992.

19. A. Dervieux, J. Malé, N. Macro, J. Périaux, B. Stoufflet, and H. Q. Chen, Some recent advances in optimal shape design for aeronautical flows, in *Proceedings of ''ECCOMAS, 2nd Computational Fluid Dynamics Conference,'' Sept. 5–8, 1994.*

20. A. Iollo and M. Salas, *Contribution to the Optimal Shape Design of Two-Dimensional Internal Flows with Embedded Shocks,* ICASE Report No. 95-20 (1995).

21. P. E. Gill, W. Murray, and M. H. Wright, *Practical Optimization,* Academic Press, San Diego, 1981.

22. M. D. Gunzburger and L. S. Hou, *Finite Dimensional Approximation of a Class of Constrained Nonlinear Optimal Control Problems,* ICASE Report No. 94-16 (1994).